Available online at www.sciencedirect.com
SCIENCE DIRECT
Virology 346 (2006) 205 – 218
VIROLOGY
www.elsevier.com/locate/yviro

EBV-encoded dUTPase induces immune dysregulation: Implications for the pathophysiology of EBV-associated disease

Ronald Glaser [a,b,c,e,*], Monica L. Litsky [b], David A. Padgett [a,b,c,d], Robert A. Baiocchi [c,e], Eric V. Yang [a,b], Min Chen [b], Peir-En Yeh [b], Kari B. Green-Church [f], Michael A. Caligiuri [a,c,e], Marshall V. Williams [a,c]

[a] *Department of Molecular Virology, Immunology and Medical Genetics, The Ohio State University Medical Center, 333 W. 10th Avenue, Columbus, OH 43210, USA*
[b] *Institute for Behavioral Medicine Research, The Ohio State University, 333 W. 10th Avenue, Columbus, OH 43210, USA*
[c] *Comprehensive Cancer Center, The Ohio State University, 300 W. 10th Avenue, Columbus, OH 43210, USA*
[d] *Department of Oral Biology, The Ohio State University, 305 W. 12th Avenue, Columbus, OH 43210, USA*
[e] *Department of Internal Medicine, The Ohio State University Medical Center, 1654 Upham Drive, Columbus, OH 43210, USA*
[f] *The Ohio State University Mass Spectrometry and Proteomics Facility, 243 Fontana Hall, 116 W. 19th Avenue, Columbus, OH 43210, USA*

Received 16 August 2005; returned to author for revision 6 October 2005; accepted 26 October 2005
Available online 29 November 2005

Abstract

Epstein–Barr virus (EBV) encodes for several enzymes that are involved in viral DNA replication. There is evidence that some viral proteins, by themselves, can induce immune dysregulation that may contribute to the pathophysiology of the virus infection. In this study, we focused on the EBV-encoded deoxyuridine triphosphate nucleotidohydrolase (dUTPase) and present the first evidence that the dUTPase is able to induce immune dysregulation in vitro as demonstrated by the inhibition of the replication of stimulated peripheral blood mononuclear cells (PBMCs) and the upregulation of several proinflammatory cytokines including TNF-α, IL-1β, IL-8, IL-6, and IL-10 produced by unstimulated PBMCs treated with purified EBV-encoded dUTPase. Depletion of CD14-positive cells (monocytes) eliminated the cytokine profile induced by EBV dUTPase treatment. The data support the hypothesis that at least one protein of the EBV early antigen complex can induce immune dysregulation and may be involved in the pathophysiology of EBV-associated disease.
© 2005 Elsevier Inc. All rights reserved.

Keywords: Monocytes/macrophages; Epstein–Barr virus; Cytokines; Tumor immunity; Cancer

Introduction

Epstein–Barr virus (EBV), a gamma herpesvirus, is the causative agent of infectious mononucleosis (IM) and is implicated in the pathogenesis of a variety of human malignancies including Burkitt's lymphoma (BL), nasopharyngeal carcinoma (NPC), Hodgkin's disease, T-cell lymphoma, and post-transplant lymphoproliferative disorder (Ablashi et al., 1990; Brousset, 2002; Petrella et al., 1997; Touitou et al., 2003). In recent years, EBV-associated malignancies have become increasingly common especially in transplant patients and patients with acquired immunodeficiency syndrome (Ho et al., 1988).

Following infection and replication of EBV in B-lymphocytes, there are changes in the secretion patterns of TNF-α, interleukin-1 (IL-1), interleukin-6 (IL-6), and interleukin-10 (IL-10) (Fayad et al., 2001; Gosselin et al., 1991, 1992a, 1992b; Tanner et al., 1996). These changes in cytokine expression and immune dysregulation are due in part to the interaction of gp350/220 (gp350), the major envelope glycoprotein encoded by EBV, and CR2, the cellular receptor for EBV on B-lymphocytes. Increases in serum levels of IL-10, IL-6, TNF-α, IL-1β, and IL-8 levels in patients with EBV-associated lymphomas have been described (Klein et al., 1996; Kurzrock, 2001; Luciani et al., 1998; Mori et al., 2003; Sharma and Zhang, 2001), and serum levels of both IL-6 and IL-10 have been correlated with disease

* Corresponding author. Institute for Behavioral Medicine Research, The Ohio State University, 333 W. 10th Avenue, 2175 Graves Hall, Columbus, OH 43210, USA. Fax: +1 614 292 1011.
E-mail address: glaser.1@osu.edu (R. Glaser).

0042-6822/$ - see front matter © 2005 Elsevier Inc. All rights reserved.
doi:10.1016/j.virol.2005.10.034

outcome in Hodgkin's disease patients with higher levels predictive of a poorer health outcome (Fayad et al., 2001; Lai et al., 2002). There is evidence that IL-10 can act as a growth factor for EBV-related tumors (Miyazaki et al., 1993). In a recent study, increased levels of IL-10 were also observed in serum from NPC patients and in the tumor cells (Budiani et al., 2002).

Cellular IL-10 is produced by Type 2 helper cells (Th-2), monocytes/macrophages, and B-cells and can inhibit the production of cytokines from Type 1 helper cells (Th-1), including interferon-gamma (IFN-γ) and IL-2 (Fiorentino et al., 1989). Because Th-1 cytokines are important for controlling virus infection, including the production of virus-specific cytotoxic T-lymphocytes targeting EBV-infected cells, this shift in the Th-1 pattern to a Th-2 pattern favors virus-induced pathogenesis.

There are recent studies which suggest that some EBV-encoded proteins can induce immune dysregulation when purified and tested in vitro. Data from one study showed that purified EBV latent membrane protein-1 (LMP-1), which is expressed in latently infected cells, was able to suppress T-cell and natural killer (NK) cell responses (Dukers et al., 2000). Another study using the purified gp350 showed that this late structural viral protein was able to upregulate TNF-α gene expression in human monocytes (D'Addario et al., 2000). Because EBV encodes for approximately 70 polypeptides, undoubtedly, more than these two (i.e., LMP-1 and gp350) will have the potential to modulate immune function.

EBV, like other herpesviruses, encodes for several enzymes that are involved in viral DNA replication; all are part of the early antigen (EA) complex. Thus far, six EBV-associated enzymes have been described. Our laboratory helped describe several of these enzymes, including the thymidine kinase (TK), DNA polymerase, deoxyribonuclease (DNase), dUTPase, and ribonucleotide reductase (Cheng et al., 1980; Glaser et al., 1973; Goodman et al., 1978; Henry et al., 1978; Miller et al., 1977; Williams et al., 1985). The EBV also encodes for a uracil–DNA glycosylase (Baer et al., 1984). Studies to determine whether any of these enzymes modulate immune function have not been performed.

In this report, we present the first evidence that the EBV-encoded dUTPase is able to induce immune dysregulation in vitro as demonstrated by its effect on the replication of PBMCs and the production of several different proinflammatory cytokines including IL-1β, TNF-α, IL-6, IL-8, and IL-10. We hypothesize that the immune dysregulation induced by EBV-encoded dUTPase, and perhaps other viral proteins, plays a role in the pathophysiology of EBV-associated disease. We provided data to support this hypothesis in a previous report, which showed that EBV-encoded dUTPase modulated immune function in mice and that these immune changes were associated with the induction of sickness behavior (Padgett et al., 2004).

Results

Purification of the EBV-encoded dUTPase

The recombinant EBV-encoded dUTPase preparations were routinely purified 450 to 750-fold using Blue Sepharose affinity chromatography followed by concentration. The identification and purity of the EBV-encoded dUTPase were assessed using mass spectrometry and proteomic-based techniques. The sample was digested using trypsin, and the peptides were analyzed using nano-LC/MS/MS. Using Mascot, the EBV-encoded dUTPase was identified with a 27% sequence coverage and a significant score of 193 where individual ion scores of >53 indicate identity or extensive homology. Trypsin was matched with a score of 88. However, trypsin was used as the proteolytic enzyme, and two autolysis peaks are commonly observed in all samples digested with trypsin. No other proteins were identified with any significance, and all interpretable MS/MS spectra were accounted for as either the EBV-encoded dUTPase or trypsin.

The total number of interpretable MS/MS spectra was eight, and the results are shown in Table 1. The peptide from amino acid 243–268 was observed as both a doubly and triply charged ion, therefore, five interpretable MS/MS spectra match sequences from the EBV-encoded dUTPase with four unique peptides matching the EBV-encoded dUTPase. A typical MS/MS spectrum of the peptides observed and sequenced on the Q-TOF™ is shown in Fig. 1. The MS/MS spectrum depicts the tryptic peptide from the solution digestion of the EBV-encoded dUTPase with *m/z* 765.5 + 2. The sequence corresponds to

Table 1
Interpretable mass spectra and the corresponding sequence from the solution digestion with trypsin of purified EBV-encoded dUTPase

Protein	Observed *m/z*	Experimental MW	Predicted MW	Δ MW	Sequence
dUTPase	765.49^{+2}	1528.96	1528.82	0.14	^{172}SGLAMQGILVKPC$_{CAM}$R^{185}
	976.10^{+2}	1950.18	1950.03	0.15	^{9}YAFQNDKLLLQQASVGR^{25}
	1021.10^{+2}	2040.18	2040.02	0.17	^{189}GGVDVSLTNFSDQTVFLNK^{207}
	923.82^{+3}	2768.45	2768.24	0.20	^{243}WATC$_{CAM}$AFEEVPGLAM$_{OX}$GDSGLSEALEGR^{268}
	1385.26^{+2}	2768.50	2768.24	0.26	^{243}WATC$_{CAM}$AFEEVPGLAM$_{OX}$GDSGLSEALEGR^{268}
Trypsin	421.80^{+2}	841.58	841.50	0.08	^{108}VATVSLPR^{115}
	737.76^{+3}	2210.26	2210.10	0.16	^{58}LGEHNIDVLEGNEQFINAAK^{77}
	1106.15	2210.30	2210.10	0.20	^{58}LGEHNIDVLEGNEQFINAAK^{77}

A total of 8 MS/MS spectra were observed with quality fragment ions, 5 account for sequences from the EBV-encoded dUTPase and 3 account for autolysis peptides from trypsin. The peptide corresponding to amino acids 243–268 is observed as both a doubly and triply charged ions making four unique peptides from the EBV-encoded dUTPase.

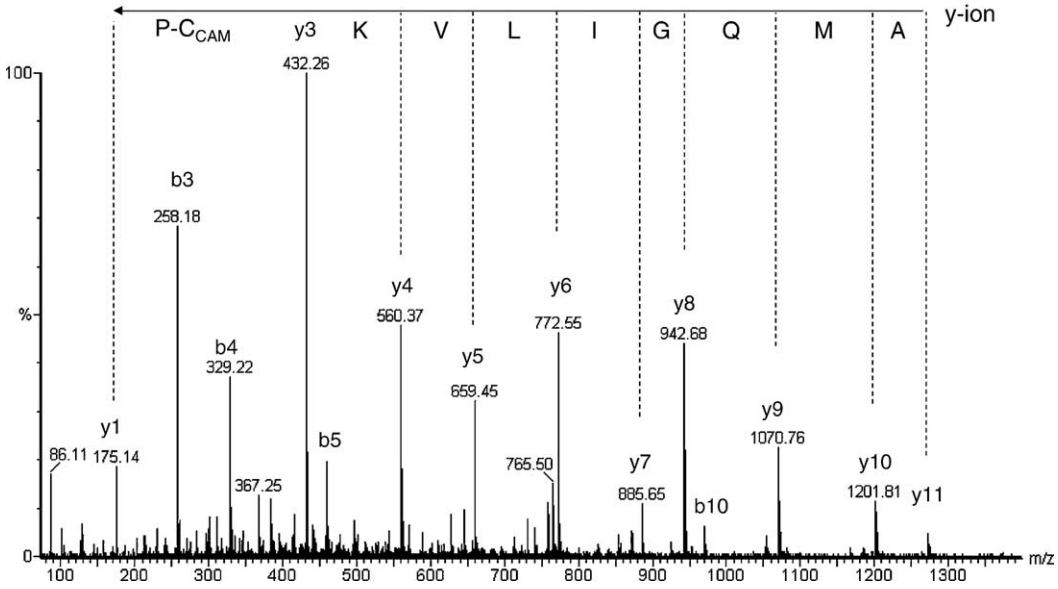

Fig. 1. MS/MS spectrum of a tryptic peptide from the solution digestion of the EBV-encoded dUTPase with m/z 765.5 + 2. The assigned b/y ions are labeled and listed in Table 2. The sequence corresponds to ^{172}SGLAMQGILVKPC$_{CAM}$R^{185}.

^{172}SGLAMQGILVKPC$_{CAM}$R^{185}. The assigned b/y ions are labeled and listed in Table 2.

EBV-encoded dUTPase has an inhibitory effect on the blastogenic response of human PBMCs stimulated with an anti-CD3 mAb

The treatment of PBMCs with the EBV-encoded dUTPase significantly inhibited anti-CD3-mAb-induced blastogenesis of cells obtained from eight individuals (two-tail $P < 0.015$ for 7.5 μg/ml and $P < 0.01$ for 15 μg/ml EBV-encoded dUTPase) (Fig. 2). Using PBMCs from three of these subjects, we found that inhibition of the blastogenic response of T-cells by EBV-encoded dUTPase was dose-dependent with saturation occurring around 1 μg/ml. Human γ-globulin was used as a non-specific protein control and did not significantly affect anti-CD3-mAb-induced blastogenesis at similar concentrations (Fig. 3).

EBV-encoded dUTPase can induce cytokine production by resting unstimulated human PBMCs

We examined EBV-encoded dUTPase-treated PBMCs for cytokine production in cell supernatants. Incubation of non-stimulated resting PBMCs with EBV-encoded dUTPase caused a rapid production/release of TNF-α that peaked at 24 h and quickly declined over time (Fig. 4A). Figs. 4B and C respectively show that EBV-encoded dUTPase can induce IL-10 and IL-1β production by human PBMCs, which reached a maximum at 24 h and slowly declined over time. IL-6 and IL-8 production was also greatly enhanced and sustained over time when the PBMCs were cultured with EBV-encoded dUTPase (Figs. 4D and E). No IL-2, IL-4, IL-5, or IL-12 p70 was detected in cell supernatants treated with the EBV-encoded dUTPase.

Although EBV dUTPase treatment of resting PBMCs induced inflammatory cytokines, IFN-γ levels in dUTPase-treated cells were not significantly different from the control cultures and were found to be within the range of 0–500 pg/ml. However, upon treatment of the cells with 0.8 μg/ml of the CD3 mAb used in the T-cell blastogenesis assay, IFN-γ levels increased 5- to 10-fold in control PBMCs cultures obtained from six out of eight individuals. Concurrent treatment of the PBMCs with EBV dUTPase and the CD3 mAb resulted in lower IFN-γ levels when compared to the control cultures from the same individuals. Two out of the eight individuals did not release any IFN-γ regardless of treatment. While the results were not statistically different, there was a trend showing that IFN-γ production was suppressed after 48 h when the PBMCs were incubated with EBV-encoded dUTPase (Fig. 4F, $P < 0.084$ for 7.5 μg/ml and $P < 0.064$ for 15 μg/ml EBV dUTPase, $n = 8$).

Table 2
Representative coverage of b and y ion series from a tryptic peptides from dUTPase corresponding to amino acid sequence 172–185

b1	b2	b3	b4	b5	b6	b7	b8	b9	b10	b11	b12	b13	b14
88.04	145.06	258.14	329.18	460.22	588.28	645.3	758.39	871.47	970.54	1098.63	1195.69	135.72	
S	G	L	A	M	Q	G	I	L	V	K	P	CCAM	R
	1442.8	1385.78	1272.69	1201.65	1070.61	942.56	885.53	772.45	659.37	560.3	432.2	335.15	175.12
	y13	y12	y11	y10	y9	y8	y7	y6	y5	y4	y3	y2	y1

Shaded boxes indicate peaks assigned have a minimum S/N ratio of 3 and are within 0.2 Da of predicted. Bold black indicates a peak assignment with a S/N at 3. In this example of the b/y ion series, 77% of the b ions are observed and 85% of y ions are observed.

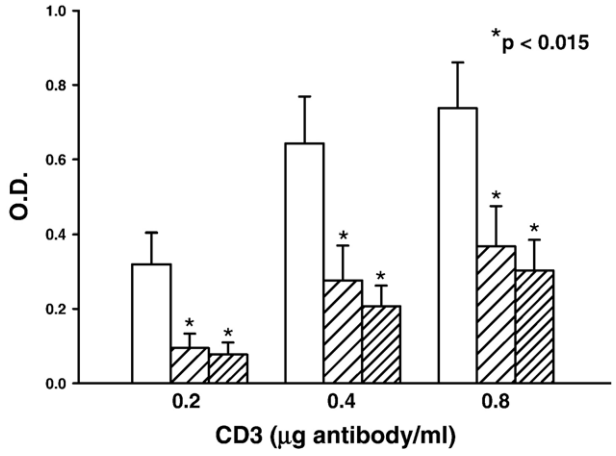

Fig. 2. The effect of EBV-encoded dUTPase on the replication of PBMCs stimulated with an anti-CD3 mAb. PBMCs were incubated for 72 h with various concentrations of an anti-CD3 mAb to induce T-cell blastogenesis. The data are presented as the change in optical density from non-stimulated and CD3-stimulated cells. The PBMCs were treated with EBV-encoded dUTPase (cross-hatched bars) at the same time the mAb was added. Results are the mean ± SEM; $n = 8$. Untreated PBMCs (▭), 7.5 μg/ml EBV dUTPase (▨), and 15 μg/ml EBV dUTPase (▨).

CD3 mAb treatment of PBMCs concurrently with the EBV dUTPase enhanced levels of TNF-α, IL-1β, IL-10, IL-,6 and IL-8 approximately two-fold when compared to dUTPase-treated PBMCs (data not shown).

Studies on the purity of the EBV dUTPase preparations

It was important to be sure that the purified EBV dUTPase preparations were not contaminated with factors, such as LPS, DNA, RNA, and peptidoglycan, that could produce the cytokine patterns observed. We had already shown that the EBV dUTPase preparations contained no other protein as determined by nano-LC/MS/MS.

Standard assays (Limulus Lysate, Quant-iT™ and SLP-HS) used for the detection and quantitation of LPS, dsDNA, RNA, and peptidoglycan demonstrated that the amount of LPS, dsDNA, RNA, or peptidoglycan was below the detection limits of these assays, which suggests that the EBV-encoded dUTPase preparations were free of these contaminates (data not shown).

In order to ensure that immunoregulatory effects were produced by the EBV-encoded dUTPase, a series of experiments were performed to demonstrate that the effects were not the result of contaminating LPS. Briefly, PBMCs were treated in a dose–response manner with LPS (0.001 to 10 μg/ml), and the supernatants examined for the production of cytokines. PBMCs were also treated with EBV-encoded dUTPase (10 μg/ml) in the presence and absence of polymyxin B (10 μg/ml); the supernatants were examined for the production of cytokines. Finally, PBMCs were treated with EBV-encoded dUTPase in the presence and absence of the 7D6 mAb, the supernatants were examined for the production of cytokines. The results for TNF-α as a representative example are shown in Fig. 5.

Treatment of the PBMCs with LPS resulted in a dose–response increase in TNF-α production (Fig. 5A). Extrapolation of the data when PBMCs from the same preparation were treated with 10 μg/ml EBV dUTPase in which 1425 pg/ml TNF-α was induced at 24 h suggests that it would take 6.2 μg/ml LPS to induce equivalent levels of TNF-α when compared to the EBV-encoded dUTPase. Based upon 1 ng LPS being equivalent to 1–10 IU, the 6.2 μg/ml LPS would be equivalent to a minimum of 620 IU of LPS/ml and would be easily detectable by the Limulus lysate assay which has a sensitivity of 0.06 IU of LPS/ml. Secondly, as shown in Fig. 5B, polymyxin B, an inhibitor of LPS, had no significant effect on TNF-α induction by the EBV-encoded dUTPase. Finally, the 7D6 mAb significantly inhibited the induction of TNF-α by the EBV-encoded dUTPase ($P < 0.025$, Fig. 5C). Similar results were obtained with the other cytokines (data not shown).

EBV-encoded dUTPase-induced cytokine profile predominately involves monocytes/macrophages

While performing the blastogenesis studies, we obtained preliminary data suggesting that the percentage of CD14+ cells in each PBMC preparation (as determined by flow cytometry) was related to the ability of the EBV-encoded dUTPase to inhibit T-cell division. Furthermore, the cytokine profile induced by EBV-encoded dUTPase treatment also suggested involvement of monocytes/macrophages. In order to test this hypothesis, we performed a series of depletion studies using MACS (see Figs. 6A–C). Removal of CD14+ cells totally eliminated the cytokine pattern observed with PBMCs treated with EBV-encoded dUTPase (Figs. 7A–E). Additionally, treatment of the adherent fraction, which was enriched for monocytes (68% CD14+ cells, Fig. 6C), with EBV-encoded dUTPase showed a cytokine profile similar to the response of

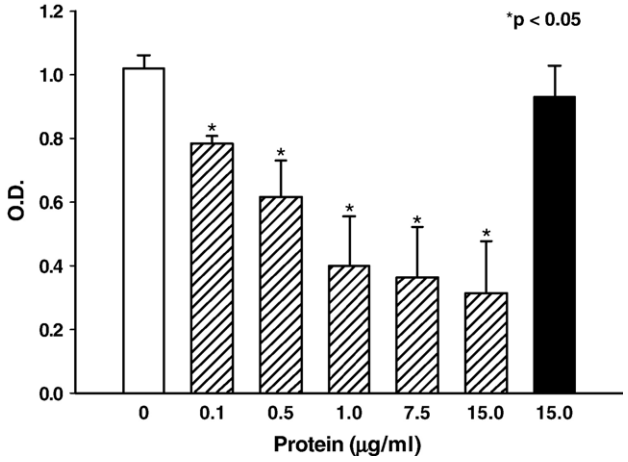

Fig. 3. Dose-dependent inhibition of the replication of PBMCs stimulated with an anti-CD3 mAb by EBV-encoded dUTPase. PBMCs were incubated with 0.8 μg/ml of an anti-CD3 mAb for 72 h as described in Materials and methods. The cells were treated with various concentrations of EBV-encoded dUTPase. The results are shown as the mean ± SEM; $n = 3$. Untreated PBMCs (▭), EBV dUTPase (▨), and human γ-globulin (■).

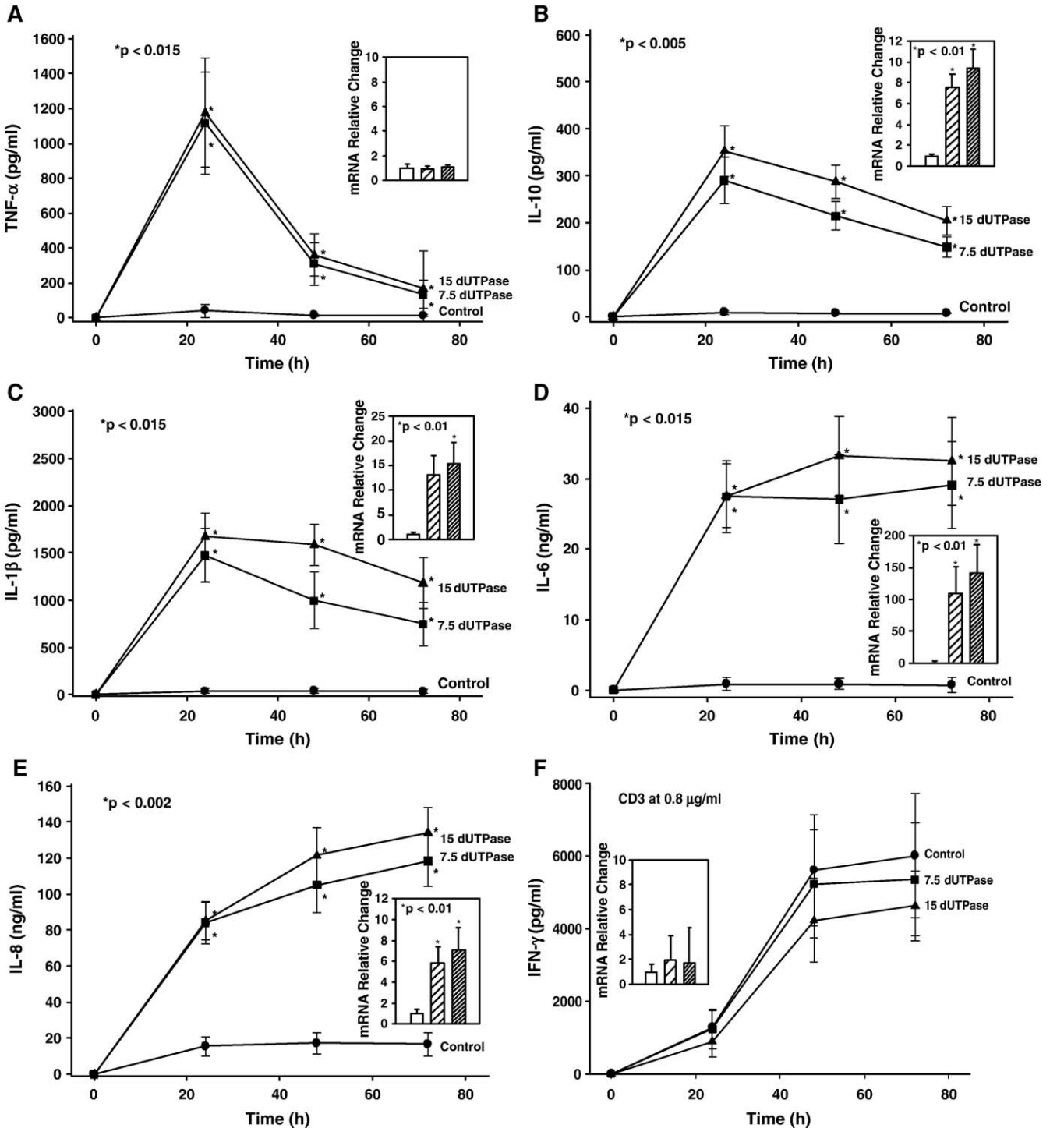

Fig. 4. (A–F) The effect of EBV-encoded dUTPase on cytokine production. PBMCs were treated with two different concentrations of EBV-encoded dUTPase as described in Materials and methods. Untreated PBMCs (●), 7.5 μg/ml EBV-encoded dUTPase (■), and 15 μg/ml EBV-encoded dUTPase (▲). Cell supernatants were assayed for cytokine levels at 24, 48, and 72 h. The results are the mean ± SEM; $n = 8$. The inserted bar-graph plots represent the relative change in cytokine mRNA expression at 24 h. Untreated PBMCs (▭), 7.5 μg/ml EBV dUTPase (▨), and 15 μg/ml EBV dUTPase (▨).

PBMCs treated with the viral protein, even though only 20% of the total cell number was used (Figs. 7A–E). We chose to test the adherent fraction to avoid any effects of the CD14 antibody on the cells. In experiments in which the adherent cells (CD14-enriched) were added back, the cytokine pattern was re-established in a concentration-dependent manner (see inserted bar-graphs within Figs. 7A–E). The enrichment of CD14+ cells by adherence was variable with each preparation. The results shown in Fig. 7 represent data obtained from the sample in which we obtained the highest purity of macrophages/monocytes. Figs. 8A–E show the correlations between the actual number of CD14+ cells added back and EBV-encoded

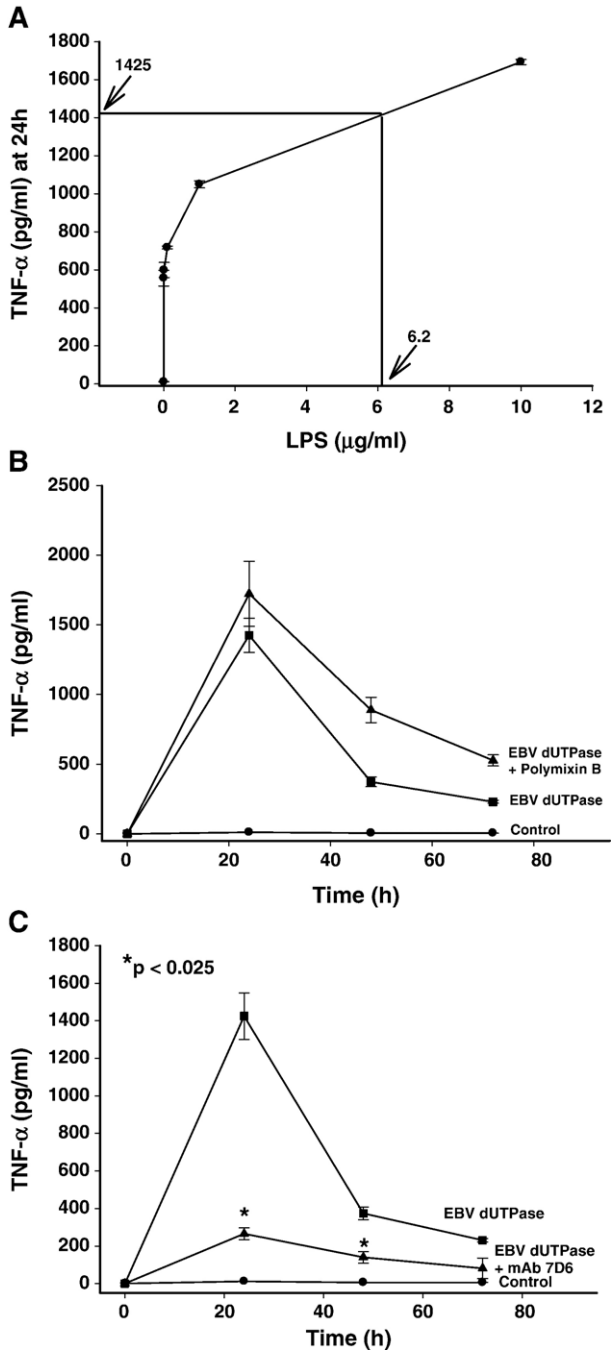

Fig. 5. (A–C) The determination of the purity of the EBV dUTPase preparations using TNF-α as the outcome measure. PBMCs were treated with 10 μg/ml EBV-encoded dUTPase as described in Materials and methods. Experiments were performed at least three times, and a typical profile is shown in this figure. The results shown are the average ± SD for duplicate assays. (A) Dose-dependent induction of TNF-α by LPS. Arrows indicate the amount of LPS needed to induce the equivalent amount of TNF-α by 10 μg/ml EBV dUTPase at 24 h. (B) Control, polymyxin B sulfate (●), EBV-encoded dUTPase (■), and EBV-encoded dUTPase plus polymyxin B sulfate (▲). (C) Control, mAb 7D6, or Rat IgG1 Isotype (●), EBV-encoded dUTPase plus rat IgG1 isotype (■), and EBV-encoded dUTPase plus mAb 7D6 (▲). Cell supernatants were assayed for cytokine levels at 24, 48, and 72 h.

dUTPase-induced cytokine production. These preliminary data suggest that monocytes/macrophages are the primary cell type being affected by the EBV-encoded dUTPase.

Discussion

While studies have demonstrated that the major capsid protein gp350 and LMP-1 of EBV modulates the immune response (D'Addario et al., 2000; Dukers et al., 2000), little is known concerning whether other EBV-encoded proteins are immunomodulatory. In this study, we demonstrate that the EBV-encoded dUTPase induces immune dysregulation. The purified protein inhibited anti-CD3-mAb-induced blastogenesis. Furthermore, the EBV-encoded dUTPase stimulated the production of cytokines in non-stimulated resting human PBMCs. The production of IL-1β, IL-6, IL-8, and IL-10 proteins was

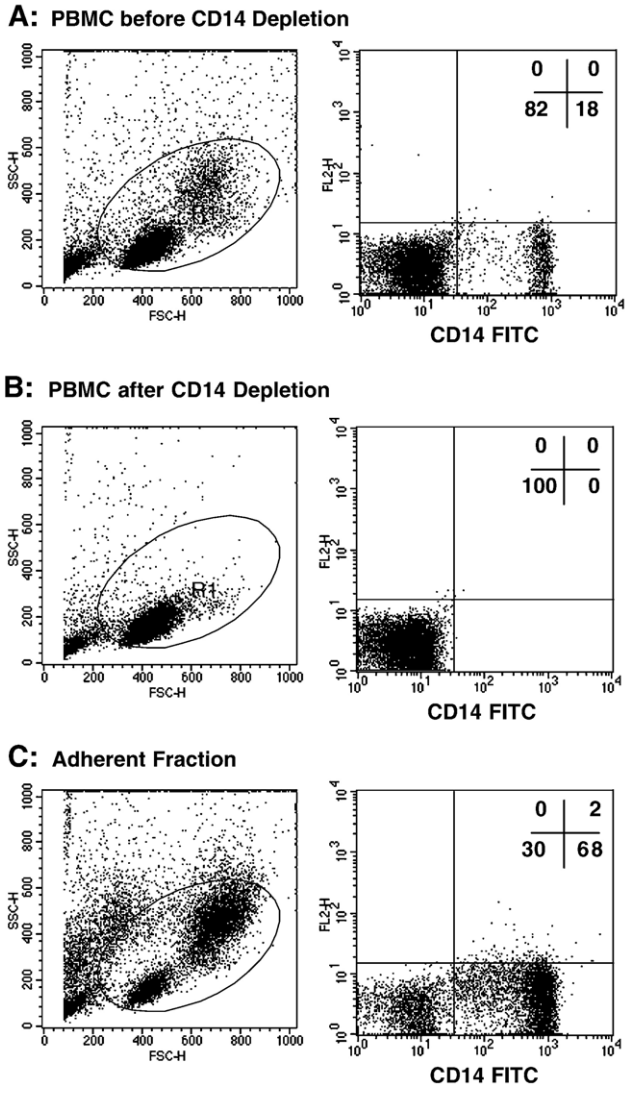

Fig. 6. (A–C) Flow cytometry analyses of CD14 depletion by MACS. CD14 depletion was performed as described in Materials and methods. Flow cytometry analysis was done using a BD FACSCalibur Flow Cytometer. Depletion and adherent experiments were performed at least three times, and a typical analysis is shown in this figure. Monocytes/macrophages are larger and have more granularity than the lymphocytes and are located in the upper right of the ellipse in the side-scatter vs. forward-scatter plot before depletion (left panel A). The monocyte/macrophage population is absent after CD14 depletion (left panel B) and enriched in the adherent fraction (left panel C). This individual's PBMCs had 18% CD14+ cells before depletion (right panel A) and none after depletion (right panel B). The adherent fraction was enriched with 68% CD14+ cells (right panel C).

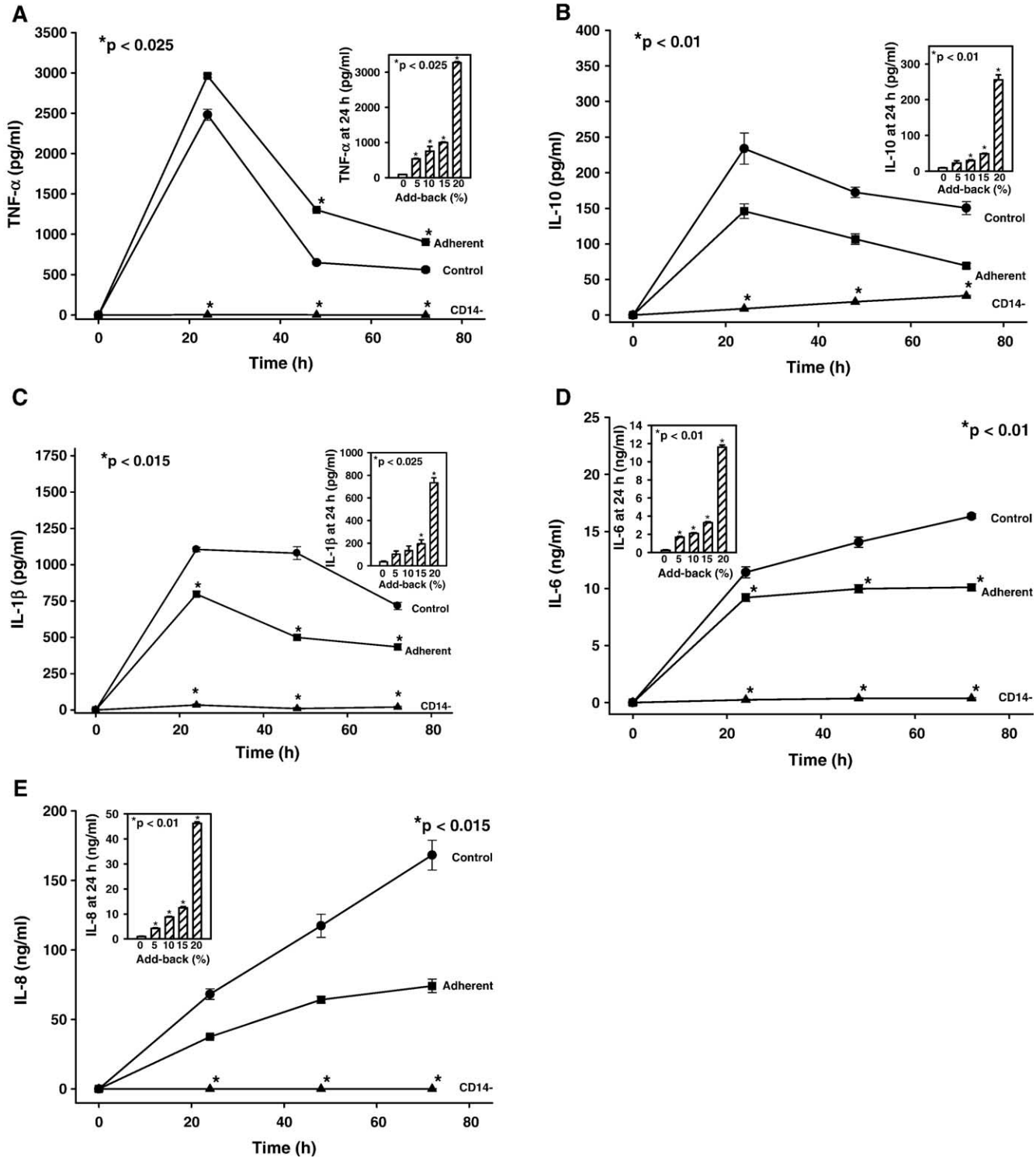

Fig. 7. (A–E) EBV-encoded dUTPase-induced cytokine profile predominately involves monocytes/macrophages. Cell fractions were treated with 10 μg/ml EBV-encoded dUTPase as described in Materials and methods. Depletion and adherent experiments were performed at least three times, and a typical profile is shown in this figure. The results shown are the average ± SD for duplicate assays. Control, PBMCs before depletion (●), adherent fraction (■), and CD14-depleted fraction (▲). Cell supernatants were assayed for cytokine levels at 24, 48, and 72 h. The inserted bar-graph plots show the change in cytokine expression at 24 h when the adherent fraction was added back to the CD14-depleted fraction (cross-hatched bars).

confirmed by an increase in mRNA levels at 24 h. Changes in TNF-α mRNA levels were detected at 3 and 6 h after dUTPase treatment. Interestingly, TNF-α was also detected by flow cytometry 3 and 6 h post-treatment at approximately 500 pg/ml and 1000 pg/ml, respectively (data not shown). The elevated TNF-α levels detected by ELISA could have resulted from de novo synthesis or release of the membrane-anchored TNF-α precursor. Although it was not our intention to perform an

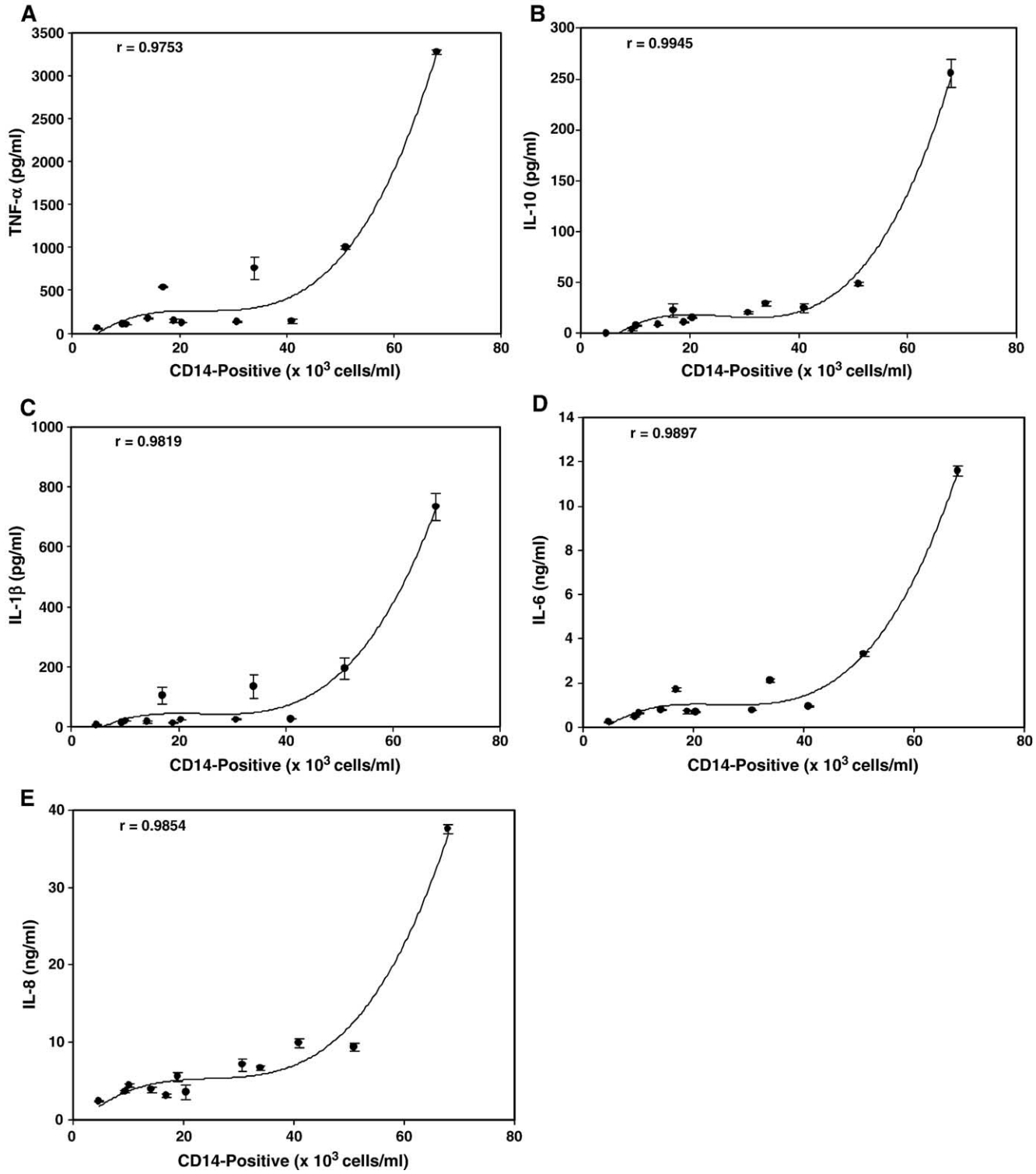

Fig. 8. (A–E) Correlation of CD14+ cells with EBV-encoded dUTPase-induced cytokine production. Cytokine production (average ± SD) was plotted against the actual number of CD14+ cells added back to the CD14-depleted fraction as determined from flow analysis of the adherent fraction. The coefficients of correlation are reported within the figures. The results were obtained from three different adherent/depleted fractions.

extensive kinetic study on the induction of cytokine expression by dUTPase, data collected at 24, 48 and 72 h allowed us to draw conclusions concerning the changes in expression over the course of treatment as compared to control cultures.

Furthermore, we demonstrate conclusively that the EBV-encoded dUTPase is responsible for inducing the immune dysfunction. Nano-LC/MS/MS was used to demonstrate that the EBV-encoded dUTPase was purified to homogeneity. To eliminate the possibility that the results of these studies with the purified EBV-encoded dUTPase were due to LPS, DNA, RNA, or peptidoglycan contamination, additional studies were performed. The Limulus lysate reaction, which has a detection

limit of 0.06 IU of LPS per ml, was negative. Assuming that the EBV-encoded dUTPase preparations were contaminated with LPS at a level of 0.05 IU per ml and that 1 IU is equivalent to 1 ng of LPS, then the maximum level of LPS that could be present in any assay was 0.03 ng or 0.03 IU. Control studies demonstrated that at least 6 μg/ml of LPS was required to induce equivalent production of TNF-α when compared to the EBV-encoded dUTPase (10 μg/ml). Furthermore, the addition of polymyxin B (10 μg/ml) did not have any effect on the ability of the EBV-encoded dUTPase to induce cytokine expression. Likewise, we demonstrated using the high sensitivity Quant-iT™ dsDNA and RNA assay systems, which have a detection limit of 1 ng/ml of dsDNA and 5 ng/ml for RNA, that the EBV-encoded dUTPase preparations were negative. Assuming that the EBV-encoded dUTPase preparations contained 0.9 ng of DNA/ml, then the maximal amount of dsDNA that could be present in any assay is 0.5 ng which is at least 3-fold less that what has been reported previously to stimulate Toll receptors (TLR) (Ahmad-Nejad et al., 2004). We also demonstrated using the SLP-HS assay, which has a detection limit of 10 pg/ml of peptidoglycan, that the EBV-encoded dUTPase preparations were free of contaminating peptidoglycan. Finally, the 7D6 mAb, which was prepared against the EBV dUTPase, prevented the induction of the cytokines by the EBV-encoded dUTPase. The results provide conclusive data demonstrating that the EBV-encoded dUTPase preparations are free of contaminating proteins, LPS, DNA, RNA, and peptidoglycan, thus further supporting our premise that the EBV-encoded dUTPase induces immune dysfunction.

The mechanism(s) through which EBV-encoded dUTPase may influence the immune response is suggested by the depletion/add-back experiments showing the role of CD14+ cells with the effect of dUTPase on PBMCs. Macrophages, as well as dendritic cells, polymorphonuclear cells, and NK cells, discriminate between foreign pathogens and self through signals mediated by pattern recognition receptors (PRR), which include the TLRs, scavenger receptors, complement receptor, members of the C-type lectin receptor family, and integrins (Fiorentino et al., 1991). TLRs recognize conserved motifs present in pathogens and when stimulated trigger a signaling cascade that leads to the activation of NF-κB and the enhanced transcription of inflammatory cytokines genes (O'Neill, 2002). Our premise is that the EBV-encoded dUTPase is a pathogen-associated molecular pattern (PAMP) that triggers a signaling cascade following its interaction with an TLR.

While the EBV-encoded dUTPase is only expressed during virus replication, there is accumulating evidence suggesting that abortive-lytic replication occurs in vitro and in vivo and that the immediate-early and early viral gene products affect cellular functions (Glaser et al., 1991, 2005). It was recently reported that EBV lytic and abortive-lytic replication occurs in plasma cells located in the tonsils of healthy individuals (Laichalk and Thorley-Lawson, 2005). Furthermore, several human herpesviruses, including EBV, are reported to infect monocytes and to undergo lytic replication in vitro (Blasig et al., 1997; Gosselin et al., 1991; Ibanez et al., 1991; Savard et al., 2000). It has been reported previously that the EBV-encoded dUTPase could be detected in epithelial cell layers of the tongue in patients with oral hairy leukoplakia and in lymphoid cells in the tonsils of patients with IM (Fleischmann et al., 2002). Likewise, antibodies to the EBV-encoded dUTPase have been detected in some patients with IM, chronic EBV infection, and HIV infection, but not in normal EBV-seropositive individuals or EBV negative subjects (Sommer et al., 1996). We now have preliminary data that show that NPC patients also have antibody to EBV-encoded dUTPase (data not shown). These results suggest that significant amounts of EBV-encoded dUTPase are expressed during lytic and/or abortive-lytic replication of EBV to affect the innate immune response.

There are reports showing that in vitro acute and persistent infections with EBV result in changes in the secretion patterns of TNF-α, IL-1, IL-6, and IL10 (Fayad et al., 2001; Gosselin et al., 1992a, 1992b; Tanner et al., 1996). There are several studies that show that increases in proinflammatory cytokines are upregulated in patients with EBV-associated diseases. Increases in serum levels of TNF-α, IL-1β, IL-6, IL-8, and IL-10 levels in patients with EBV-associated lymphomas have been described (Klein et al., 1996; Kurzrock, 2001; Luciani et al., 1998; Mori et al., 2003; Sharma and Zhang, 2001), and serum levels of both IL-6 and IL-10 have been correlated with disease outcome in Hodgkin's disease patients with higher levels predictive of a poorer health outcome (Fayad et al., 2001; Lai et al., 2002). IL-10 which is produced by activated monocytes and T- and B-cell lymphomas can inhibit the production of IL-1, IL-2, IL-6, and IFN-γ (Mosmann, 1994). The EBV also encodes for a viral IL-10 (V-IL10), a homologue to cellular IL-10; VIL-10 can inhibit the production of IFN-γ and IL-1. This cytokine pattern would result in favoring the survival of EBV since IL-10 can inhibit the induction of EBV-specific cytotoxic T-cells to latent EBV-infected growth and malignantly transformed cells (Kanno et al., 1997; Rickinson et al., 1992). It is of interest that, in a recent study, increased levels of IL-10 were also observed in serum from NPC patients and in the NPC tumor cells (Budiani et al., 2002).

We have also shown that the EBV-encoded dUTPase can induce immune dysregulation in vivo in mice. Confirming the results from this in vitro study, EBV-encoded dUTPase inhibited mitogen-stimulated blastogenesis of lymph node and spleenic-derived lymphocytes recovered from mice inoculated with EBV-encoded dUTPase. Decrements in the synthesis of IFN-γ were also observed. Importantly, the mice inoculated with the dUTPase demonstrated sickness behavior known to be induced by some of the same cytokines that were found to be upregulated in this study. Compared to control mice, the dUTPase-treated mice lost body mass, had elevated body temperatures, and diminished locomotor activity (Padgett et al., 2004).

In summary, there is evidence in the literature to support the hypothesis that viral proteins, by themselves, can induce immune dysregulation. For example, the 15e kDa polypeptide of the feline leukemia virus (FeLV) significantly inhibits replication of mitogen-stimulated feline lymphocytes in vitro (Mathes et al., 1979). Furthermore, a recombinant peptide, HIV-1 env–gag, suppressed the synthesis of IgG by pokeweed mitogen-treated human B-lymphocytes; the same recombinant

peptide significantly increased the proliferative response of PBMCs as compared with control cultures (Nair et al., 1988). As already discussed, data from two recent studies show that purified EBV LMP-1 and gp350 can induce immune dysregulation (D'Addario et al., 2000; Dukers et al., 2000). These viral-encoded proteins are either capsid/envelope components or are expressed on the membranes of latently infected cells. In contrast, the EBV-encoded dUTPase is a non-structural EA protein.

As already discussed, patients with specific clinical histories have unique antibody patterns to several EBV-encoded enzymes including the dUTPase. The mechanism(s) underlying the process that results in such antibody patterns is not known. The availability of these EBV early proteins to induce an antibody response would result from the lysis of cells in which the latent EBV genome was fully reactivated. It is also possible that early proteins like the dUTPase can be released by cells undergoing abortive reactivation (Deng et al., 2004; Glaser et al., 1991, 2005). In such cells, an early protein(s), e.g., viral encoded enzyme(s), may be synthesized and expressed on the surface of the cell as an HLA-restricted immunodominant target for CTLs and be capable of inducing an antibody response (Steven et al., 1997).

The data presented in this paper and the paper in which the EBV-encoded dUTPase was shown to induce sickness behavior in mice (Padgett et al., 2004) provide a new perspective on the role of an EBV-encoded early non-structural protein in the pathophysiology of EBV-associated disease. Whether other early proteins can induce immune dysregulation needs to be explored. However, the data from this study and others (D'Addario et al., 2000; Dukers et al., 2000; Mathes et al., 1979; Nair et al., 1988) show that at least some of the viral-encoded proteins can produce changes in both humoral and cellular immunity separate from their roles in virus replication/latency. The data may have implications for understanding the role of EBV and other herpesviruses in diseases/syndromes of unknown etiology, such as chronic fatigue syndrome (Glaser et al., 2005; Gotleib-Stematsky and Glaser, 1982).

Materials and methods

Purification of EBV-encoded dUTPase

The EBV-encoded dUTPase gene (BLLF3) was cloned into a pET3A vector, which was kindly provided by Peter Sommer (Institut fur Mikrobiologic und Hygiene, Abteilung Virolgie). The plasmid was maintained in *E. coli* (BL21EBVdUT) using ampicillin (100 μg/ml) selection. The EBV-encoded dUTPase (Mr = 31 kDa) was purified to apparent homogeneity using Blue Sepharose affinity chromatography. Briefly, BL21EBV-dUT was grown in LB medium containing chloramphenicol (25 μg/ml) and ampicillin (100 μg/ml) at 37 °C for 2.5 h. IPTG (1 mM final concentration) was added, and the culture was incubated an additional 2 h at 37 °C. Bacteria were collected from 6 l of medium by low speed centrifugation, and the bacterial pellet was resuspended in 50 ml of extraction buffer (10 mM Tris–HCL, pH 7.5, 1 mM $MgCl_2$, 2 mM 2-mercaptoethanol, and a protease inhibitor cocktail containing antipain, benzamidine, chymostatin, leupeptin, pepstatin, TLCK, and TPCK at a final concentration 1 μg/ml each). Bacteria were lysed by ultrasonication. The resulting homogenate was centrifuged (15,000×g, 30 min at 4 °C), and the supernatant was applied to a Blue Sepharose (Sigma Chemical Co.) column (2.5 × 25 cm) equilibrated with extraction buffer. The matrix was washed with equilibration buffer and equilibration buffer containing 1 M NaCl (500 ml each), and the EBV-encoded dUTPase was eluted using a linear gradient of 1 M to 2 M NaCl in equilibration buffer.

Under these conditions, the *E. coli* dUTPase is not retained on the matrix, while the EBV-encoded dUTPase is retained and begins to elute at approximately 1.6 M NaCl. Fractions containing maximal dUTPase activity were combined and concentrated using Centriprep-30 (Amicon, Beverly, MA). EBV-encoded dUTPase activity was determined as described previously using the DE81 filter disc assay (Cheng et al., 1980). A unit of dUTPase activity was defined as the amount of enzyme required to convert 1 nmol of dUTP to dUMP and pyrophosphate per min at 37 °C under the assay conditions. The specific activity of the EBV-encoded dUTPase preparations used in these studies ranged from 450 to 750 units/mg of protein. Protein concentration was determined with the Coomassie Brilliant Blue dye-binding assay (Bio-Rad Laboratories) using bovine serum albumin as the standard. To rule out endotoxin contamination in our protein preparations, dUTPase preparations were assayed for endotoxin using the Limulus Amebocyte Lysate Kit (BioWhittaker), which can detect an endotoxin concentration of 0.06 IU/ml.

Several additional assays were performed to eliminate the possibility that our purified EBV-encoded dUTPase preparations were contaminated with other bacterial components such as DNA, RNA, and peptidoglycan. High sensitivity Quant-iT™ kits (Molecular Probes) were used to detect possible DNA and RNA contamination. The Quant-iT™ DNA HS assay can detect double-stranded (ds) DNA down to 1 ng/ml, while the Quant-iT™ RNA assay has a detection limit of 5 ng/ml. For the detection of peptidoglycan, the silkworm larvae plasma (SPL) assay (Wako Chemicals) was employed. The SLP assay not only detects peptidoglycan but also β-glucan, a cell wall component of fungi. The SLP-HS assay has a detection limit of 10 pg/ml of peptidoglycan. The purified EBV-encoded dUTPase, which was stored at 4 °C at stock concentrations of 0.5 and 1 mg/ml, was used for these studies.

The purity of EBV-encoded dUTPase was determined by capillary-liquid chromatography–nanospray tandem mass spectrometry (nano-LC/MS/MS). Briefly, the EBV-encoded dUTPase was digested essentially as described previously (Russell et al., 2001). The EBV-encoded dUTPase preparation was desalted using manual syringe protein traps (Michrom BioResources; Auburn, CA) and resuspended in 10 μl of water. Dithiothreitol (5 μl of a 5 mg/ml solution in 100 mM ammonium bicarbonate) was added to reduce the cysteines. The solution was heated at 50 °C for 15 min, cooled, and iodoacetamide (5 μl of a 15 mg/ml solution in 100 mM ammonium bicarbonate) was added and reacted in the dark at room temperature for 15 min. Sequencing grade trypsin (20 ng/

ml in 50 mM acetic acid; Promega, Madison WI) was added at 1:25 trypsin to EBV-encoded dUTPase, and the final buffer conditions for digestion were 25 mM ammonium bicarbonate and 40% acetonitrile. The digestion was performed at 37 °C for 4 h and stopped by acidification with 1 μl of trifluoroacetic acid.

Nano-LC/MS/MS was performed on a Micromass, a hybrid quadrupole time-of-flight Q-TOF™ II (Micromass, Wythenshawe, UK) mass spectrophotometer equipped with an orthogonal nanospray source (New Objective, Inc., Woburn, MA) operated in positive ion mode. The LC system was an UltiMate Plus System (LC-Packings) with a Famous autosampler and Switchos column switcher. Solvent A was water containing 50 mM acetic acid, and Solvent B was acetonitrile. Each sample (2.5 μl) was first injected on the trapping column and then washed with 50 mM acetic acid. The peptides were eluted off the trap onto the column, and an ID ProteoPep C18 column (5 cm, 75 μM; New Objectives, Inc.) packed directly in the nanospray tip was used for chromatographic separations. Peptides were eluted from the column into the Q-TOF™ system using a gradient of 2–80% Solvent B over 50 min with a flow rate of 300 nl/min. A total run time was 55 min. The nanospray capillary voltage was set a 3.0 kV and the cone voltage at 55 V. The source temperature was maintained at 100 °C. Mass spectra were recorded using MassLynx 4.0 with automatic switching functions. Mass spectra were acquired from mass 400 to 2000 Da every second with a resolution of 8000 (FWHM). When the desired peak (using included tables) was detected at a minimum of 15 ion counts, the mass spectrophotometer automatically switched to acquire CID MS/MS spectrum of the individual peptides. Collision energy was set dependent on charge state recognition properties. Sequence information from the MS/MS data was processed using Mascot Distiller (http://www.Matrixscience.com/). Database searches were performed using Mascot from Matrix Science and PEAKS from Bioinformatics Solutions.

Sequence information from the MS/MS data was processed using Mascot Distiller to form a peaklist (.mgf file). Data processing was performed following established guidelines (Carr et al., 2004). Briefly, data were minimally processed, a 3-point smooth was applied, and the centroid was calculated from the top 80% of the peak height. The charge state of each ion selected for MS/MS was calculated, however, the peaks were not deisotoped. Assigned peaks have a minimum of 5 counts (S/N of 3) and must show the corresponding C13 ion to be considered valid. The mass accuracy of the precursor ions was set to 1.2 Da to accommodate accidental selection of the C13 ion, and the fragment mass accuracy was set to 0.3 Da. Considered modifications (variable) were methionine oxidation and carbamidomethyl cysteine. NCBInr was the database used in the search.

The effect of EBV-encoded dUTPase on human T-cell replication and cytokine production

In order to determine if EBV-encoded dUTPase affected human T-cell replication and function in vitro, experiments were performed with PBMCs obtained from the American Red Cross from healthy donors through an Ohio State University-approved IRB protocol. We did not determine if the subjects who provided the blood samples were latently infected with EBV and, therefore, seropositive for the virus. However, since we showed in a previous study that approximately 90% of adults are seropositive for EBV, it is probable that most, if not all, of our subjects were seropositive (Glaser et al., 1985).

PBMCs were isolated by density gradient centrifugation using Histopaque-1077 (Sigma) by routine procedures. To induce T-cell proliferation, PBMCs (0.5×10^6 cells/ml) were treated with an anti-CD3 monoclonal antibody (mAb) (Coulter Clone UCHT1) for 72 h in the presence of either 7.5 μg/ml or 15 μg/ml of purified EBV-encoded dUTPase (total volume 0.1 ml). For negative controls, cells were treated with buffer or human γ-globulin, which was used as a non-specific protein control as described in previous studies (D'Addario et al., 2000; Dukers et al., 2000; Nair et al., 1988; Voo et al., 2002).

Blastogenesis was measured using the CellTiter 96 Aqueous Non-Radioactive Cell Proliferation Assay (Promega) using samples in triplicate. The O.D. value obtained from unstimulated PBMCs ± protein was subtracted from the O.D. value from CD3-stimulated PBMCs ± protein. For cytokine studies (total volumes ranged from 0.2 to 1 ml, depending on the cytokine), cell cultures were set up in polystyrene round-bottom tubes at the same cellular and EBV-encoded dUTPase concentrations used in the blastogenesis assay. Supernatants were harvested for cytokine analysis at 24, 48, and 72 h. The cell pellets were resuspended in 0.8 ml Trizol (Invitrogen Life Technologies) for RNA isolation. Real-time RT-PCR was performed to measure mRNA levels.

In order to confirm that the observed cytokine induction profile was a direct result of the EBV-encoded dUTPase and not LPS contamination, polymyxin B sulfate (Sigma) was added at 10 μg/ml in the presence or absence of 10 μg/ml EBV dUTPase; supernatants were harvested over a 72 h period as indicated above. Additionally, neutralization studies were performed in which a mAb to the EBV-encoded dUTPase 7D6 (Nicholls et al., 1998) or a rat IgG1 isotype was preincubated at room temperature with 10 μg/ml EBV dUTPase for 1 h prior to treatment of PBMCs; the supernatants were harvested and tested for cytokine analysis as indicated above.

Cytokine analysis

Concentrations of different cytokines in cell culture supernatants of resting non-stimulated PBMCs exposed to 7.5 μg/ml or 15 μg/ml of the EBV-encoded dUTPase were measured with commercially available human cytokine ELISA kits or by flow cytometry. Buffer-treated cells were used as negative controls. Specifically, IL-2, IL-4, and IL-5 concentrations were measured using the Human Th-1/Th-2 Cytokine Cytometric Bead Array Kits (BD Biosciences). IL-1β, IL-6, IL-8, IL-10, IL-12p70, and TNF-α concentrations were measured with the Human Inflammation Cytometric Bead Array Kits (BD Biosciences). IFN-γ

concentrations were determined using ELISA kits purchased from Biosource International. The minimal detectable concentration for each cytokine is as follows: 6.6 pg/ml for IL-2; 6.5 pg/ml for IL-4; 2.8 pg/ml for IL-5; 7.2 pg/ml for IL-1β; 2.5 pg/ml for IL-6; 3.6 pg/ml for IL-8; 3.3 pg/ml for IL-10; 1.9 pg/ml for IL-12p70; 3.7 pg/ml for TNF-α; and 4 pg/ml for IFN-γ.

Real-time RT-PCR analysis

mRNA levels of IL-6, IL-10, IL-8, IL-1β, TNF-α, and IFN-γ were measured using real-time RT-PCR analysis on total RNA obtained from PBMCs treated with EBV-encoded dUTPase for 24 h and from control cultures. Total RNA from PBMCs was extracted with Trizol reagent (Invitrogen Life Technologies) according to the manufacturer's suggested protocol. The genomic DNA was sheared in the sample by passing twice through a 26-gauge needle connected to a 1 ml syringe. Total RNA was precipitated with isopropanol in the presence of glycogen (Roche Applied Science) at 200 μg/ml as a carrier. The total RNA pellet was resuspended in RNAse-free water (Ambion) and stored at −80 °C until analysis.

RNA was reverse-transcribed from 500 ng of total RNA with random hexamers and Superscript II (Invitrogen Life Technologies). Real-time RT-PCR was performed using the Rotor-Gene sequence detector (Corbett Research). The cycle parameters for the PCR were set up according to the manufacturer's suggestion. Gene-specific primers and probes (TaqMan PDARS) for IL-1β, IL-6, IL-8, IL-10, IFN-γ, and GAPDH were purchased from Applied Biosystems; the TNF-α primer and probe were gifts from Michael Caliguiri. Relative quantitations of cytokine mRNA expression were calculated with the comparative C_t method. Each target cytokine value was divided by the endogenous reference GAPDH value to obtain a normalized target value.

Depletion analysis

Based on our preliminary results, which suggested the involvement of macrophages/monocytes (CD14+ cells), we performed experiments to remove CD14+ cells from PBMCs using Magnetic Cell Sorting (MACS) Microbeads (Miltenyi Biotec, Germany). Depletion of CD14+ cells was performed according to the manufacturer's instructions. Briefly, 9 ml of PBMCs at approximately 6×10^6 cells/ml was plated onto a 150 × 25 mm polystyrene tissue culture plate for 4 h at 37 °C/5% CO_2. Non-adherent cells were gently washed from the plate with Ca^{2+}/Mg^{2+}-free PBS, incubated with CD14 Microbeads at the manufacturer's suggested concentration, washed, and applied successively to two LS Separation Columns (Miltenyi Biotec, Germany). Column flow-through was analyzed by flow cytometry to confirm removal of the specific cell type using CD14-FITC (Miltenyi Biotec Clone TÜK4). An adherent fraction was also collected from the tissue culture plate after incubating with Ca^{2+}/Mg^{2+}-free PBS at 4 °C for an hour. CD14-depleted non-adherent cells (0.5×10^6 cells/ml) and adherent cells (0.1×10^6) were treated with 10 μg/ml EBV-encoded dUTPase over 72 h for cytokine analysis. Additional experiments were conducted in which the adherent cells were added back to the CD14-depleted population at a percentage of total non-adherent cells (i.e., 1×10^5 adherent cells represented 20% of 5×10^5 CD14-depleted non-adherent cells) and treated with 10 μg/ml EBV-encoded dUTPase over 72 h for cytokine analysis. The number of CD14+ cells varied per adherent preparation; the actual number of CD14+ cells added back was determined from flow analysis of the adherent fraction.

Statistical analysis

Statistical analyses were performed using a paired two-sample *t* test for the means. Results are shown as the mean ± SEM. Two-tailed *P* values are reported when significant ($P < 0.05$). Nonlinear regression analysis was performed using Tukey's cubic transformations. The coefficients of correlation (*r*) are reported within the figures. Further analysis revealed that 75–83% of the residuals fell within ±1 S_e and 100% within ±2 S_e.

Acknowledgments

We thank Rich Gandour and J. Dennis Pollack for their input and excellent suggestions for the manuscript. We also thank Stephanie Dickinson for her help on statistical analyses. This study was supported by grants AG16321, DE13749 (NIH), and The Gilbert and Kathryn Mitchell Endowment and The Ohio State University Comprehensive Cancer Center core grant CA16058 (NCI).

References

Ablashi, D.V., Huang, A.T., Pagano, J.S., Pearson, G.R., Yang, C.S., 1990. Epstein–Barr Virus and Human Disease. Humana Press, Clifton, NJ.

Ahmad-Nejad, P., Mrabet-Dahbi, S., Breuer, K., Klotz, M., Werfel, T., Herz, U., Heeg, K., Neumaier, M., Renz, H., 2004. The toll-like receptor 2 R753Q polymorphism defines a subgroup of patients with atopic dermatitis having severe phenotype. J. Allergy Clin. Immunol. 113 (3), 565–567.

Baer, R., Bankier, A.T., Biggin, M.D., Deininger, P.L., Farrell, P.J., Gibson, T.J., Hatfull, G., Hudson, G.S., Satchwell, S.C., Seguin, C., 1984. DNA sequence and expression of the B95-8 Epstein–Barr virus genome. Nature 310 (5974), 207–211.

Blasig, C., Zietz, C., Haar, B., Neipel, F., Esser, S., Brockmeyer, N.H., Tschachler, E., Colombini, S., Ensoli, B., Sturzl, M., 1997. Monocytes in Kaposi's sarcoma lesions are productively infected by human herpesvirus 8. J. Virol. 71 (10), 7963–7968.

Brousset, P., 2002. The Epstein–Barr virus infection relevant in lymphomagenesis? Hum. Pathol. 33 (2), 143–145.

Budiani, D.R., Hutahaean, S., Haryana, S.M., Soesatyo, M., Sosroseno, W., 2002. Interleukin-10 levels in Epstein–Barr virus-associated nasopharyngeal carcinoma. J. Microbiol. Immunol. Infect. 35 (4), 265–268.

Carr, S., Aebersold, R., Baldwin, M., Burlingame, A., Clauser, K., Nesvizhskii, A., 2004. The need for guidelines in publication of peptide and protein identification data: working group on publication guidelines for peptide and protein identification data. Mol. Cell. Proteomics 3 (6), 531–533.

Cheng, Y.C., Chen, J.Y., Hoffman, P.J., Glaser, R., 1980. Studies on the activity of DNase associated with the replication of the Epstein–Barr virus. Virology 100, 334–338.

D'Addario, M., Ahmad, A., Morgan, A., Menezes, J., 2000. Binding of the Epstein–Barr virus major envelope glycoprotein gp350 results in the upregulation of the TNF-alpha gene expression in monocytic cells via NF-

kappaB involving PKC, PI3-K and tyrosine kinases. J. Mol. Biol. 298, 765–778.
Deng, J.H., Zhang, Y.J., Wang, X.P., Gao, S.J., 2004. Lytic replication-defective Kaposi's sarcoma-associated herpesvirus: potential role in infection and malignant transformation. J. Virol. 78 (20), 11108–11120.
Dukers, D.F., Meij, P., Vervoort, M.B., Vos, W., Scheper, R.J., Meijer, C.J., Bloemena, E., Middeldorp, J.M., 2000. Direct immunosuppressive effects of EBV-encoded latent membrane protein 1. J. Immunol. 165 (2), 663–670.
Fayad, L., Keating, M.J., Reuben, J.M., O'Brien, S., Lee, B.-N., Lerner, S., Kurzrock, R., 2001. Interleukin-6 and interleukin-10 levels in chronic lymphocytic leukemia: correlation with phenotypic characteristics and outcome. Blood 97 (1), 256–263.
Fiorentino, D.F., Bond, M.W., Mosmann, T.R., 1989. Two types of mouse T. Helper Cell IV. Th2 clones secrete a factor that inhibits cytokine production by Th1 clones. J. Exp. Med. 170, 2081–2095.
Fiorentino, D.F., Zlotnik, A., Mosmann, T.R., Howard, M., O'Garra, A., 1991. IL-10 inhibits cytokine production by activated macrophages. J. Immunol. 147, 3815–3822.
Fleischmann, J., Kremmer, E., Greenspan, J.S., Grasser, F.A., Niedobitek, G., 2002. Expression of viral and human dUTPase in Epstein–Barr virus-associated diseases. J. Med. Virol. 68, 568–573.
Glaser, R., Ogino, T., Zimmerman Jr., J., Rapp, F., 1973. Thymidine kinase activity in Burkitt lymphoblastoid somatic cell hybrids after induction of the EB virus. Proc. Soc. Exp. Biol. Med. 142, 1059–1062.
Glaser, R., Strain, E.C., Tarr, K., Holliday, J.E., Donnerberg, R.L., Kiecolt-Glaser, J.K., 1985. Changes in Epstein–Barr virus antibody titers associated with aging. Proc. Soc. Exp. Biol. Med. 179, 352–355.
Glaser, R., Pearson, G.R., Jones, J.F., Hillhouse, J., Kennedy, S., Mao, H.Y., Kiecolt-Glaser, J.K., 1991. Stress-related activation of Epstein–Barr virus. Brain Behav. Immun. 5 (2), 219–232.
Glaser, R., Litsky, M.L., Padgett, D.A., Baiocchi, R.A., Yang, E.V., Chen, M., Yeh, P.-E., Klimas, N.G., Marshall, G.D., Whiteside, T., Herberman, R., Williams, M.V., 2005. Stress-associated changes in the steady state expression of latent Epstein–Barr virus: implications for chronic fatigue syndrome and cancer. Brain Behav. Immun. 19 (2), 91–103.
Goodman, S.R., Prezyna, C., Benz, W.C., 1978. Two Epstein–Barr virus-associated DNA polymerase activities. J. Biol. Chem. 253 (23), 8617–8628.
Gosselin, J., Menezes, J., D'Addario, M., Hiscott, J., Flamand, L., Lamoureux, G., Oth, D., 1991. Inhibition of tumor necrosis factor-alpha transcription by Epstein–Barr virus. Eur. J. Immunol. 21, 203–208.
Gosselin, J., Flamand, L., D'Addario, M., Hiscott, J., Menezes, J., 1992a. Infection of peripheral blood mononuclear cells by herpes simplex and Epstein–Barr viruses: differential induction of interleukin-6 and tumor necrosis factor alpha. J. Clin. Invest. 89, 1849–1856.
Gosselin, J., Flamand, L., D'Addario, M., Hiscott, J., Stefanescu, I., Ablashi, D.V., Gallo, R.C., Menezes, J., 1992b. Modulatory effects of Epstein–Barr, herpes simplex and human herpes-6 viral infections and co-infections on cytokine synthesis: a comparative study. J. Immunol. 149, 181–187.
Gotleib-Stematsky, T., Glaser, R., 1982. Association of Epstein–Barr virus with neurologic diseases. In: Glaser, R., Gotlieb-Stematsky (Eds.), Human Herpesvirus Infections Clinical Aspects. Marcel Dekker, Inc., New York, NY, pp. 169–204.
Henry, B.E., Glaser, R., Hewetson, J., O'Collaghan, D., 1978. Expression of altered ribonucleotide reductase activity associated with the replication of the Epstein–Barr virus. Virology 89, 262–271.
Ho, M., Jaffe, R., Miller, G., Breinig, M.K., Dummer, J.S., Makowka, L., Atchison, R.W., Karrer, F., Nalesnik, M.A., Starzl, T.E., 1988. The frequency of Epstein–Barr virus infection and associated lymphoproliferative syndrome after transplantation and its manifestations in children. Transplantation 45 (4), 719–727.
Ibanez, C.E., Schrier, R., Ghazal, P., Wiley, C., Nelson, J.A., 1991. Human cytomegalovirus productively infects primary differentiated macrophages. J. Virol. 65 (12), 6581–6588.
Kanno, H., Naka, N., Yasunaga, Y., Luchi, K., Yamauchi, S., Hashimoto, M., Aozasa, K., 1997. Production of the immunosuppresive cytokine interleukin-10 by Epstein–Barr-virus-expressing pyothorax-associated lymphoma. Possible role in the development of overt lymphoma in immunocompetent hosts. Am. J. Pathol. 150 (1), 349–357.
Klein, S.C., Kube, D., Abts, H., Diehl, V., Tesch, H., 1996. Promotion of IL8, IL10, TNF alpha and TNF beta production by EBV infection. Leuk. Res. 20 (8), 633–636.
Kurzrock, R., 2001. Cytokine deregulation in cancer. Biomed. Pharmacother. 55 (9–10), 543–547.
Lai, R., O'Brien, S., Maushouri, T., Rogers, A., Kantarjian, H., Keating, M., Albitar, M., 2002. Prognostic value of plasma interleukin-6 levels in patients with chronic lymphocytic leukemia. Cancer 95 (5), 1071–1075.
Laichalk, L.L., Thorley-Lawson, D.A., 2005. Terminal differentiation into plasma cells initiates the replicative cycle of Epstein–Barr virus in vivo. J. Virol. 79 (2), 1296–1307.
Luciani, M.G., Stoppacciaro, A., Peri, G., Mantovani, A., Ruco, L.P., 1998. The monocyte chemotactic protein a (MCP-1) and interleukin 8 (IL-8) in Hodgkin's disease and in solid tumours. Mol. Pathol. 51 (5), 273–276.
Mathes, L.E., Olsen, R.G., Hebebrand, L.C., Hoover, E.A., Schaller, J.P., Adams, P.W., Nichols, W.S., 1979. Immunosuppressive properties of a virion polypeptide, a 15,000-dalton protein from feline leukemia virus. Cancer Res. 39 (3), 950–955.
Miller, R., Glaser, R., Rapp, F., 1977. Studies of an Epstein–Barr virus-induced DNA polymerase. Virology 76, 494–502.
Miyazaki, I., Cheung, R.K., Dosch, H.-M., 1993. Viral interleukin 10 is critical for the induction of B cell growth transformation by Epstein–Barr virus. J. Exp. Med. 178, 439–447.
Mori, A., Takao, S., Pradutkanchana, J., Kietthubthew, S., Mitarnun, W., Ishida, T., 2003. High tumor necrosis factor-alpha levels in patients with Epstein–Barr virus-associated peripheral T-cell proliferative disease/lymphoma. Leuk. Res. 27 (6), 493–498.
Mosmann, T.R., 1994. Properties and functions of interleukin-10. Adv. Immunol. 56, 1–26.
Nair, M.P.N., Pottathil, R., Heimer, E.P., Schwartz, S.A., 1988. Immunoregulatory activities of human immunodeficiency virus (HIV proteins): effect of HIV recombinant and synthetic peptides on immunoglobulin synthesis and proliferative responses by normal lymphocytes. Proc. Natl. Acad. Sci. U. S. A. 85, 6498–6502.
Nicholls, J.M., Sommer, P., Kremmer, E., Ong, K.S., Fung, K., Lee, J.M., Ng, M.H., Grasser, F.A., 1998. A new lytic antibody, 7D6, detects Epstein–Barr virus dUTPase in nonkeratinizing undifferentiated nasopharyngeal carcinomas. Lab. Invest. 78 (8), 1031–1032.
O'Neill, L.A., 2002. Signal transduction pathways activated by the IL-1 receptor/toll-like receptor superfamily. Curr. Top. Microbiol. Immunol. 270, 47–61.
Padgett, D.A., Hotchkiss, A.K., Pyter, L.M., Nelson, R.J., Yang, E., Yeh, P.-E., Litsky, M., Williams, M., Glaser, R., 2004. Epstein–Barr Virus-encoded dUTPase modulates immune function and induces sickness behavior in mice. J. Med. Virol. 74, 442–448.
Petrella, T., Yaziji, N., Colin, F., Rifle, G., Morlevat, F., Arnould, L., Fargeot, P., Depret, O., 1997. Implication of the Epstein–Barr virus in the progression of chronic lymphocytic leukaemia/small lymphocytic lymphoma to hodgkin-like lymphomas. Anticancer Res. 17, 3907–3914.
Rickinson, A.B., Murray, R.J., Brooks, J., Griffin, H., Moss, D.J., Masucci, M.G., 1992. T cell recognition of Epstein–Barr virus associated lymphomas. Cancer Surv. 13, 53–80.
Russell, W.K., Park, Z.Y., Russell, D.H., 2001. Proteolysis in mixed organic–aqueous solvent systems: applications for peptide mass mapping using mass spectrometry. Anal. Chem. 73, 2682–2685.
Savard, M., Belanger, C., Tardif, M., Gourde, P., Flamand, L., Gosselin, J., 2000. Infection of primary human monocytes by Epstein–Barr virus. J. Virol. 74 (6), 2612–2619.
Sharma, V., Zhang, L., 2001. Interleukin-8 expression in AIDS-associated lymphoma B-cell lines. Biochem. Biophys. Res. Commun. 282 (2), 369–375.
Sommer, P., Kremmer, E., Bier, S., Konig, S., Zalud, P., Zeppezauer, M., Jones, J.F., Mueller-Lantzsch, N., Grasser, F.A., 1996. Cloning and expression of the Epstein–Barr Virus encoded dUTPase: patients with acute, reactivated or chronic virus infection develop antibodies against the enzyme. J. Gen. Virol. 77 (Pt. 11), 2795–2805.
Steven, N.M., Annels, N.E., Kumar, A., Leese, A.M., Kurilla, M.G., Rickinson,

R.-F., 1997. Immediate early and early lytic cycle proteins are frequent targets of the Epstein–Barr virus-induced cytotoxic T cell response. J. Exp. Med. 185 (9), 1605–1617.

Tanner, J.E., Alfieri, C., Chatil, T.A., Diaz-Mitoma, F., 1996. Induction of interleukin-6 after stimulation of human B-cell CD21 by Epstein–Barr virus glycoproteins gp350 and gp220. J. Virol. 70, 570–575.

Touitou, R., Arbach, H., Cochet, C., Feuillard, J., Martin, A., Raphael, M., Joab, I., 2003. Heterogeneous Epstein–Barr virus latent gene expression in AIDS-associated lymphomas and in type I Burkitt's lymphoma cell lines. J. Gen. Virol. 84, 949–957.

Voo, K.S., Fu, T., Heslop, H.E., Brenner, M.K., Rooney, C.M., Wang, R.-F., 2002. Identification of HLA-DP3-restricted peptides from EBNA1 recognized by CD4 (+) T cells. Cancer Res. 62 (24), 7195–7199.

Williams, M.V., Holliday, J.E., Glaser, R., 1985. Induction of a deoxyuridine triphosphate nucleotidohdrolase activity in Epstein–Barr virus-infected cells. Virology 142, 326–333.